Letter

Equation of state of a hot-and-dense quark gluon plasma: Lattice simulations at real μ_B vs extrapolations

Szabolcs Borsányi,[1] Zoltán Fodor,[1,2,3,4,5] Matteo Giordano,[4] Jana N. Guenther,[1] Sándor D. Katz,[4,6] Attila Pásztor,[4,*] and Chik Him Wong[1]

[1]*Department of Physics, Wuppertal University, Gaussstrasse 20, D-42119 Wuppertal, Germany*
[2]*Department of Physics, Pennsylvania State University, State College, Pennsylvania 16801, USA*
[3]*Jülih Supercomputing Centre, Forschungszentrum Jülich, D-52425 Jülich, Germany*
[4]*ELTE Eötvös Loránd University, Institute for Theoretical Physics, Pázmány Péter sétány 1/A, H-1117 Budapest, Hungary*
[5]*Physics Department, USDA, San Diego, California 92093, USA*
[6]*MTA-ELTE Theoretical Physics Research Group, Pázmány Péter sétány 1/A, H-1117 Budapest, Hungary*

(Received 19 September 2022; accepted 14 March 2023; published 15 May 2023)

The equation of state of the quark gluon plasma is a key ingredient of heavy-ion phenomenology. In addition to the traditional Taylor method, several novel approximation schemes have been proposed with the aim of calculating it at finite baryon density. In order to gain a pragmatic understanding of the limits of these schemes, we compare them to direct results at $\mu_B > 0$, using reweighting techniques free from an overlap problem. We use 2stout improved staggered fermions with eight time slices and cover the entire Relativistic Heavy Ion Collider Beam Energy Scan range in the baryochemical potential, up to $\mu_B/T = 3$.

DOI: 10.1103/PhysRevD.107.L091503

I. INTRODUCTION

The equation of state (EOS) of QCD matter under extreme conditions–high temperatures or baryon densities—plays a role in many physical systems, such as the early Universe, heavy-ion collisions, and neutron stars. The most established first-principles method to study the strongly coupled regime is lattice QCD [1], which maps the path integral formulation to a classical statistical-mechanical system, suitable for simulation with Monte Carlo methods. Many properties of strongly interacting matter at zero density have been elucidated using this method, such as the crossover nature of the transition [2], the transition temperature [3,4], and the EOS [5,6]. Studies at finite density are, however, hampered by the sign problem: the Boltzmann weights in the path integral representation become complex, preventing importance sampling. Thus, most lattice results on hot-and-dense QCD matter use extrapolations from zero [7–17] or purely imaginary chemical potential [18–33], situations with no sign problem.

In spite of the difficulties, there has recently been considerable progress on the EOS of the quark gluon plasma (QGP). First, Taylor coefficients of the pressure p in the baryochemical potential μ_B have been calculated up to fourth order in the continuum [11,12,14] and up to eighth order at finite lattice spacing [17,26,31]—albeit with large uncertainties at sixth and eighth order. Second, resummation schemes have been proposed for the Taylor expansion [34–38], with a promise of better convergence. At the moment there is no theoretical understanding of the convergence properties of these schemes. It is therefore important for phenomenology to determine the region of validity of these techniques. This is the purpose of this work. To this end, we use novel developments in simulation techniques for finite density: Reweighting schemes where the pressure difference between the simulated and target theories can be calculated without encountering heavy-tailed distributions—i.e., an overlap problem. Recently, such studies have become feasible for improved lattice actions with physical quark masses for two schemes: sign reweighting and phase reweighting [39,40]. These have the advantage of giving direct, reliable results at $\mu_B > 0$—provided that the exponential sign problem is dealt with by sufficient statistics. By comparing the EOS calculated using phase reweighting with the Taylor expansion and its resummations, we can quantify the systematic bias of the different truncations of these schemes, giving unprecedented insight into the EOS.

We simulate 2stout improved staggered fermions with physical quark masses on lattices with eight time

*Corresponding author.
apasztor@bodri.elte.hu

slices—a discretization that is often used as the first or second point of continuum extrapolations of thermodynamic quantities [2,5,24,30,41–46]. Cutoff effects on the EOS are moderate (after applying a tree-level improvement [5]). We reimplement all discussed extrapolations using this setup. Thus, differences can only come from the systematics of the extrapolation. Since we are interested in a comparison of various methods for a statistical physics system, the physical volume can be chosen freely. We use a fixed aspect ratio of $LT = 2$, with T the temperature and L the spatial size. As we perform no finite volume scaling, we must restrict ourselves to the study of the QGP EOS, leaving that of the fate of the crossover transition to a later date.

II. OBSERVABLES

The grand partition function of lattice QCD is given schematically by

$$Z(T,\mu) = \int \mathcal{D}U \det \mathrm{M}(U,\mu) e^{-S_g(U)}, \tag{1}$$

where $S_g(U)$ is the gauge action, $\det \mathrm{M}$ is the quark determinant, implicitly including all flavors, as well as staggered rooting, μ collectively denotes the chemical potentials of all quark flavors, and U are the link variables. We work with the quark chemical potentials $\mu_q \equiv \mu_u = \mu_d$ and $\mu_s = 0$. We concentrate on the pressure as a function of the temperature and dimensionless chemical potential $\hat{\mu}_B \equiv \mu_B/T = 3\mu_q/T \equiv 3\hat{\mu}_q$, given by

$$\hat{p}(T,\hat{\mu}_B) \equiv \frac{p(T,\hat{\mu}_B)}{T^4} = \frac{1}{(LT)^3} \ln Z(T,\hat{\mu}_B). \tag{2}$$

In particular, we study the pressure difference between zero and nonzero chemical potentials,

$$\Delta\hat{p} = \frac{\Delta p}{T^4} \equiv \hat{p}(T,\hat{\mu}_B) - \hat{p}(T,0). \tag{3}$$

We also compute the light quark density,

$$\hat{n}_L(T,\hat{\mu}_B) \equiv \frac{\mathrm{d}\hat{p}}{\mathrm{d}\hat{\mu}_B} = \frac{1}{3(LT)^3} \left(\frac{\partial \ln Z(T,\hat{\mu}_B)}{\partial \hat{\mu}_q} \right)_{\mu_s=0}. \tag{4}$$

The integral of $\hat{n}_L$ over $\hat{\mu}_B$ is $\Delta\hat{p}$. We calculate the EOS with several methods.

III. REWEIGHTING FROM $\mu_B = 0$

In what is arguably the simplest reweighting scheme, simulations are performed at $\mu_B = 0$ and $\Delta\hat{p}$ is reconstructed via [47]

$$\Delta\hat{p}(T,\hat{\mu}_B) = \frac{1}{(LT)^3} \ln \left\langle \frac{\det \mathrm{M}(\hat{\mu}_B)}{\det \mathrm{M}(0)} \right\rangle_{\hat{\mu}_B=0}. \tag{5}$$

While Eq. (5) is exact with infinite statistics, the tails of the distribution of the weights $\frac{\det \mathrm{M}(\hat{\mu}_B)}{\det \mathrm{M}(0)}$ are heavy and so hard to sample (overlap problem). It is therefore hard to judge the reliability of results from this method. It was proposed that the overlap problem can be mitigated by reweighting in more parameters [48–50]. However, even with multiparameter reweighting, the overlap problem remains the main bottleneck (at least around the transition line [51]). We include results from (one-parameter) reweighting from $\mu_B = 0$ for completeness, and because one of the resummations we will test can be regarded as a truncation of this scheme.

IV. PHASE REWEIGHTING

A way to avoid heavy-tailed distributions in the weights is to simulate a theory where these can only take values in a compact domain. Two examples are sign reweighting [39,40,52,53] and phase reweighting [40,54,55]. Here we use the latter: In the simulated theory one replaces the quark determinant with its absolute value. This is the phase quenched ensemble, corresponding to a finite isospin chemical potential, i.e., $\mu_u = -\mu_d$. The pressure schematically reads

$$\hat{p}_I(T,\hat{\mu}_q) = \frac{1}{(LT)^3} \log \int \mathcal{D}U |\det \mathrm{M}| e^{-S_g}. \tag{6}$$

It is also given by the integral of the isospin density,

$$\hat{n}_I(T,\hat{\mu}_q) \equiv \left(\frac{\partial \hat{p}_I}{\partial \hat{\mu}_q} \right)_{\mu_s=0}, \tag{7}$$

from which the pressure at finite μ_B is obtained as

$$\hat{p}(T,\hat{\mu}_B = 3\hat{\mu}_q) - \hat{p}_I(T,\hat{\mu}_q) = \frac{1}{(LT)^3} \ln \langle e^{i\theta} \rangle_{PQ}, \tag{8}$$

where $e^{i\theta} = \frac{\det \mathrm{M}(\hat{\mu}_B)}{|\det \mathrm{M}(\hat{\mu}_B)|}$ is the complex phase factor of the fermion determinant and $\langle \ldots \rangle_{PQ}$ means taking an expectation value in the phase quenched theory. Finally,

$$\Delta\hat{p} = \int_0^{\hat{\mu}_B/3} \hat{n}_I(\hat{\mu}_q, T) \mathrm{d}\hat{\mu}_q + \frac{1}{(LT)^3} \ln \langle e^{i\theta} \rangle_{PQ}. \tag{9}$$

Alternatively, one can calculate $\hat{n}_L$ directly,

$$\hat{n}_L = \frac{1}{(LT)^3 \langle e^{i\theta} \rangle_{PQ}} \left\langle e^{i\theta} \frac{\partial}{\partial \hat{\mu}_B} \ln \det \mathrm{M} \right\rangle_{PQ}, \tag{10}$$

from which $\Delta\hat{p}$ is obtained via integration. The two methods are not guaranteed to give compatible results if the observable in the numerator of Eq. (10), namely $e^{i\theta} \frac{\partial}{\partial \hat{\mu}_B} \ln \det \mathrm{M}$, has an overlap problem. This is possible,

as only the pressure difference $p(T,\hat{\mu}_B=\hat{\mu}_q)-p_I(T,\hat{\mu}_I=\hat{\mu}_q)\propto\langle e^{i\theta}\rangle_{PQ}$ in Eq. (8) is guaranteed to be free of one—due to the compactness of $e^{i\theta}$.

The phase diagram at finite isospin density was calculated in Ref. [45]. It has a pion condensed phase for low T and $\mu_q > m_\pi/2$. In this region, the sign problem is severe. Here we avoid this issue by concentrating on the EOS of the QGP, and we find a mild sign problem: $\langle e^{i\theta}\rangle_{PQ}=\langle\cos\theta\rangle_{PQ}$ never gets below 0.1 in any of our ensembles and is always more than 10σ away from zero.

V. TAYLOR EXPANSION

The pressure is expanded in powers of the baryochemical potential,

$$\hat{p}(T,\hat{\mu}_B)=p_0(T)+p_2(T)\hat{\mu}_B^2+p_4(T)\hat{\mu}_B^4+\ldots. \quad (11)$$

We calculate the Taylor coefficients two ways: by using configurations generated at $\mu_B=0$ to calculate them directly and by using simulations at imaginary μ_B to obtain them from a fit. These are the procedures used in the literature so far. For a recent example of the first, see, e.g., Ref. [17], and for the second, Refs. [26,31].

VI. RESUMMATIONS BASED ON SHIFTING SIGMOID FUNCTIONS

A resummation of the Taylor expansion was introduced in Ref. [34], defined implicitly via

$$\frac{\hat{n}_L(T,\hat{\mu}_B)}{\hat{\mu}_B}=\frac{\mathrm{d}\hat{n}_L}{\mathrm{d}\hat{\mu}_B}(T(1+\kappa_2(T)\hat{\mu}_B^2+\ldots),0). \quad (12)$$

This is motivated by the empirical observation of the existence of an approximate scaling variable $T(1+\kappa\hat{\mu}_B^2)$, coming from lattice studies at imaginary chemical potential: Certain observables collapse on single (sigmoid shaped) curves when plotted against this variable [33,34]. Up to $\hat{\mu}_B=1.5$ the existence of an approximate scaling variable has also been confirmed directly at a real μ_B by sign reweighting [40]. This is the $\frac{\hat{n}_L(T,\hat{\mu}_B)}{\hat{\mu}_B}$ shifting method. This is a systematically improvable expansion. Its validity is not predicated on the existence of this approximate scaling variable, but if an approximate scaling variable exists, we expect the method to converge fast.

A disadvantage of the previous scheme is that it was designed to work near the crossover. To make it more suitable for high T, it was later refined [38] by introducing a Stefan-Boltzmann correction,

$$\frac{\hat{n}_L(T,\hat{\mu}_B)}{\hat{n}_L^{\mathrm{SBL}}(\hat{\mu}_B)}=\lim_{\hat{\mu}_B'\to 0}\frac{\hat{n}_L(T(1+\lambda_2\hat{\mu}_B^2+\ldots),\hat{\mu}_B')}{\hat{n}_L^{\mathrm{SBL}}(\hat{\mu}_B')}, \quad (13)$$

where we introduced the Stefan-Boltzmann limit (SBL),

$$\hat{n}_L^{\mathrm{SBL}}(\hat{\mu}_B)\equiv\lim_{T\to\infty}\hat{n}_L(T,\hat{\mu}_B). \quad (14)$$

We call this method the $\frac{\hat{n}_L(T,\hat{\mu}_B)}{\hat{n}_L^{\mathrm{SBL}}}$ shifting method. Both shifting methods can be implemented by fitting the κ_n or λ_n coefficients to data at imaginary μ_B.

VII. EXPONENTIAL RESUMMATION

A different resummation is based on truncating the reweighting from $\mu_B=0$ [35], by approximating $\frac{\det \mathrm{M}(\hat{\mu}_B)}{\det \mathrm{M}(0)}\simeq\exp\left(\sum_{n=1}^{N}\frac{1}{n!}\mathcal{D}_n\hat{\mu}_B^n\right)$ in Eq. (5),

$$\Delta\hat{p}(T,\hat{\mu}_B)\simeq\frac{1}{(LT)^3}\ln\left\langle\exp\left(\sum_{n=1}^{N}\frac{1}{n!}\mathcal{D}_n\hat{\mu}_B^n\right)\right\rangle_{\hat{\mu}_B=0}, \quad (15)$$

where $\mathcal{D}_n\equiv\frac{\partial^n}{\partial\hat{\mu}_B^n}\ln\ \det \mathrm{M}(\hat{\mu}_B)$ and N is the truncation order. A practical advantage is that the coefficients $\mathcal{D}_n$ are needed for the calculation of the Taylor coefficients p_{2n} anyway. Thus, this scheme represents an alternative way to analyze data for the Taylor coefficients. The procedure introduced in Ref. [35] had the disadvantage of using a biased estimator for Eq. (15), by exponentiating the stochastic estimators of the $\mathcal{D}_n$. This bias was studied in Ref. [36]. We remove this bias by calculating the $\mathcal{D}_n$ exactly for each configuration, using the reduced matrix formalism [56].

VIII. LATTICE SETUP AND NUMERICAL RESULTS

We used a tree-level Symanzik improved gauge action and two steps of stout smearing [57] with $\rho=0.15$ on the links entering the quark determinant, with physical quark masses, using the kaon decay constant for scale setting [58]. We apply a tree-level improvement factor to the pressure, making the $N_\tau=8$ 2stout results close to the continuum [5]. This corresponds to division by 1.28 at infinite volume, which is the correction we apply for in $\hat{n}_L$ and $\Delta\hat{p}$.

We study $16^3\times 8$ lattices at various temperatures with $145\le T\le 240$ MeV and light quark chemical potential $\mu_u=\mu_d=\mu_q=\mu=\mu_B/3$ with a zero strange quark chemical potential $\mu_s=0$, corresponding to a strangeness chemical potential $\mu_S=\mu_B/3$.

We simulate the phase quenched ensemble for $\hat{\mu}_B^2=1.5$, 3, 4.5, 6, 7.5, and 9, without an explicit symmetry breaking term, commonly used at a finite isospin density [45,59]. Instead, we follow the method of Ref. [40]. The resulting ensemble corresponds to an isospin chemical potential $\mu_I=\mu_u=-\mu_d$. We use these ensembles to reweight to a baryochemical potential with $\mu_u=\mu_d=\mu_B/3$. Determinant ratios are calculated using the reduced matrix [56,60]. We performed the calculation of $\Delta\hat{p}$ in two inequivalent

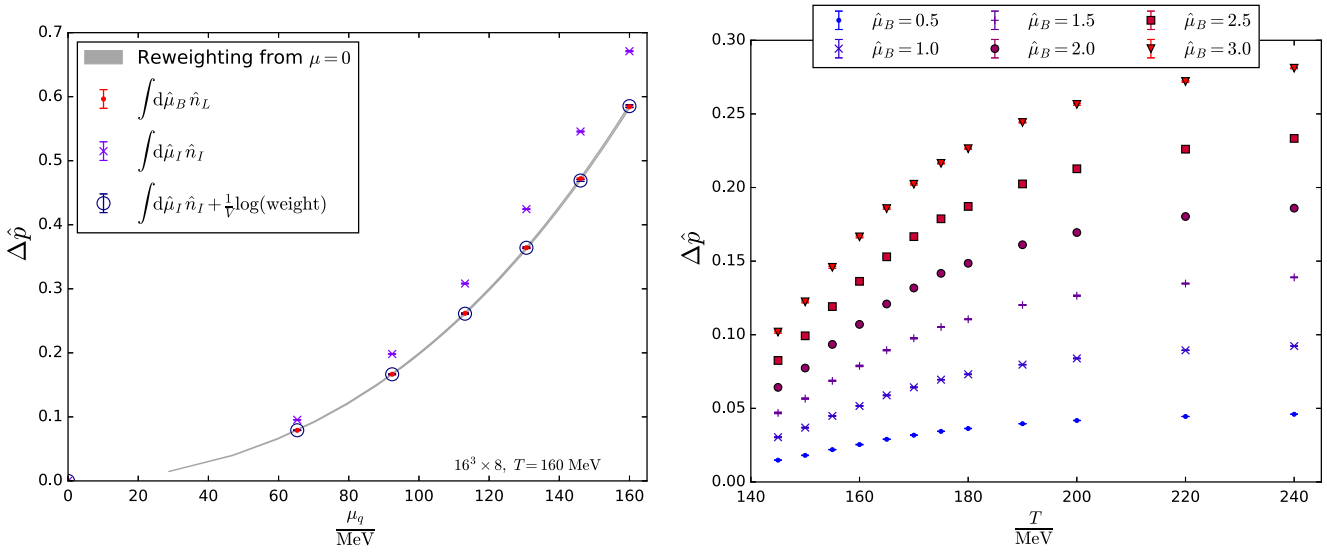

FIG. 1. Left: the pressure difference between the zero and nonzero chemical potential theory calculated with several different reweighting methods as a function of the quark chemical potential at $T = 160$ MeV. Results at finite isospin chemical potential are shown as purple points. The nonzero isospin data are direct results in the phase quenched ensemble, obtained without reweighting. Results reweighted from the phase quenched ensemble to finite μ_B with the two methods discussed in the text are shown by red and blue points. Results from reweighting from zero μ_B are shown in gray. Right: the pressure difference between zero and nonzero baryochemical potentials, calculated with phase reweighting as a function of T, for different values of $\hat{\mu}_B$.

ways: the one with no possible overlap problem described by Eq. (9) and by integration of Eq. (10). We obtain compatible results for $\Delta\hat{p}$ with both methods, as can be seen in Fig. 1 (left) for $T = 160$ MeV.

We also simulate $\mu_B = 0$ for $T/\text{MeV} = 140$, 150, 160, and 170 to perform reweighting from $\mu_B = 0$, to calculate the Taylor coefficients and exponential resummation. For all of these, we used the reduced matrix formalism [56], so obtaining the Taylor coefficients without the use of stochastic estimators and obtaining $\mathcal{D}_n$ exactly for each configuration, encountering no bias in the exponentiation [35,36].

In Fig. 1 (left) we also show the results for $\Delta\hat{p}$ from reweighting from $\mu_B = 0$. These results are also in agreement with the two ways of reweighting from the phase quenched ensemble for all temperatures in our study.

Three different reweighting procedures—including one with no possible overlap problem—give identical results. This strongly supports the validity of our results for the EOS. The full results for $\Delta\hat{p}$ from phase reweighting are shown in Fig. 1 (right). We can safely use these results to test extrapolations.

Without comparison with phase reweighting, we could not guarantee the correctness of reweighting from $\mu_B = 0$, due to the overlap problem. This problem is inherited by the Taylor method: Since the expansion coefficients of the pressure are obtained by Taylor expanding the logarithm of the reweighting factor, i.e., $\langle \frac{\det M(\mu_B)}{\det M(0)} \rangle$, for any finite ensemble the Taylor coefficients are exactly the Taylor coefficients of the reweighted pressure, as opposed to the exact pressure. Thus, if the reweighted pressure with a given statistics has a systematic bias due to an overlap problem, so will the Taylor coefficients. By showing that reweighting from $\mu_B = 0$ works for the region $\hat{\mu}_B \leq 3$, we ensure that we are truly testing the convergence of the Taylor series, without encountering an overlap problem in the higher order coefficients.

IX. COMPARISON WITH EXTRAPOLATION SCHEMES

To implement the resummation schemes based on shifting sigmoids, we perform simulations at imaginary chemical potentials, for $\text{Im}\,\hat{\mu}_B \frac{16}{\pi} = 0$, 4, 6, 7, 8, 9, 10, and 12. We work to order κ_4 in Eq. (12) and to order λ_4 in Eq. (13), using a simplified version of the analysis of Refs. [34,38]. The systematic error includes the fit range in imaginary μ_B, the ansatz in μ_B^2, and the interpolation of the light quark susceptibility at $\mu_B = 0$. As a more straightforward use of the imaginary chemical potential data we perform a second determination of the Taylor coefficients, fitting $\frac{\hat{n}_L}{\hat{\mu}_B}$ with a polynomial of order $\hat{\mu}_B^6$. For the fits we also include $\frac{d^2\hat{p}}{d\hat{\mu}_B^2}$ and $\frac{d^4\hat{p}}{d\hat{\mu}_B^4}$ at $\mu_B = 0$ as further data points.

We show the comparison of extrapolation schemes with the direct data in Fig. 2, as a function of T at a fixed $\hat{\mu}_B = \sqrt{7.5}$ and 3 (the two largest values where we have direct data) and in Fig. 3 as a function of the chemical potential at fixed temperatures of $T = 160$ MeV and 170 MeV. The Taylor expansion at next-to-leading order (NLO)—$\mathcal{O}(\mu_B^4)$ in the pressure—is not consistent with the direct data,

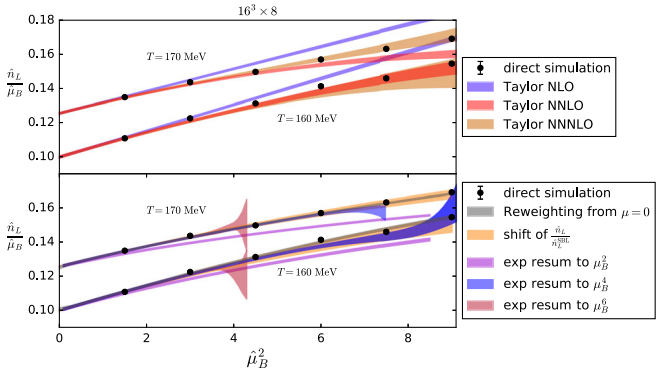

FIG. 2. The direct results for $\hat{n}_L$ at nonzero μ_B compared with different approximations: the Taylor method and the exponential resummation (exp resum) [35] to different orders calculated from the ensemble at $\mu_B = 0$, as well as the shifting $n_L/n_L^{\rm SBL}$ method calculated from imaginary chemical potential simulations and reweighting from $\mu_B = 0$.

systematically underestimating n_L below 150 MeV and overestimating it above 150 MeV. This is due to a peak in $p_4(T)$ slightly above the crossover temperature. Including the $p_6(T)$ term, the Taylor method agrees with the direct data up to $\hat{\mu}_B = 3$ at $T = 160$ MeV and up to $\hat{\mu}_B \approx 1.2$ at $T = 170$ MeV. Including the next-to-next-to-next-to-leading order (NNNLO) term $p_8(T)$, the expansion agrees with the direct data at all studied temperatures up to $\hat{\mu}_B = 3$.

In contrast, exponential resummation shows bad convergence properties from $\hat{\mu}_B^2 \approx 4$ for all temperatures. While the $N = 2$ truncation remains close to the direct results in the entire range, higher orders make the agreement better only below this value.

At large T, the method based on shifting $\hat{n}_L/\hat{n}_L^{\rm SBL}$ outperforms the method of shifting $\hat{n}_L/\hat{\mu}_B$. This is expected, as the Stefan-Boltzmann correction was introduced [38] to improve the scheme at high T.

Thus, both the Taylor expansion to order $\hat{\mu}_B^8$ and the resummation based on shifting $\hat{n}_L/\hat{n}_L^{\rm SBL}$ to order λ_4 accurately describe the equation of state in the range $0 \le \hat{\mu}_B \le 3$—the entire range of the RHIC Beam Energy Scan. Note the faster convergence of the resummation, as the calculation of λ_4 only requires determining the Taylor coefficients up to order $\hat{\mu}_B^6$. On the other hand, the shifting $\hat{n}_L/\hat{\mu}_B$ method at order κ_4 has a slight systematic discrepancy with the direct data at large T, and exponential resummation shows bad convergence properties above $\hat{\mu}_B^2 \approx 4$.

X. DISCUSSION

We judged the reliability of different approximation schemes by comparing them with direct results for $0 \le \hat{\mu}_B \le 3$. This gives a practical answer to the question of which approximations to trust. A theoretical understanding of the reasons would also be welcome. For schemes defined in terms of thermodynamic quantities, such as the Taylor expansion or the resummations based on shifting sigmoids, this requires knowledge of partition function (Lee-Yang) zeros in the complex μ_B plane [16,37,60–62]. Exponential resummation, instead, is not defined in terms of thermodynamic quantities, but by manipulating the integrand of the path integral. Understanding its convergence also requires understanding nuances of the path integral, in addition to thermodynamic singularities. We speculate that the limited convergence is due to quark determinant zeros: The sum in the argument of the exponential in Eq. (15) approximates the quark effective action in a fixed gauge field background, with a radius of convergence determined by the determinant zeros, leading to logarithmic divergences. These are not

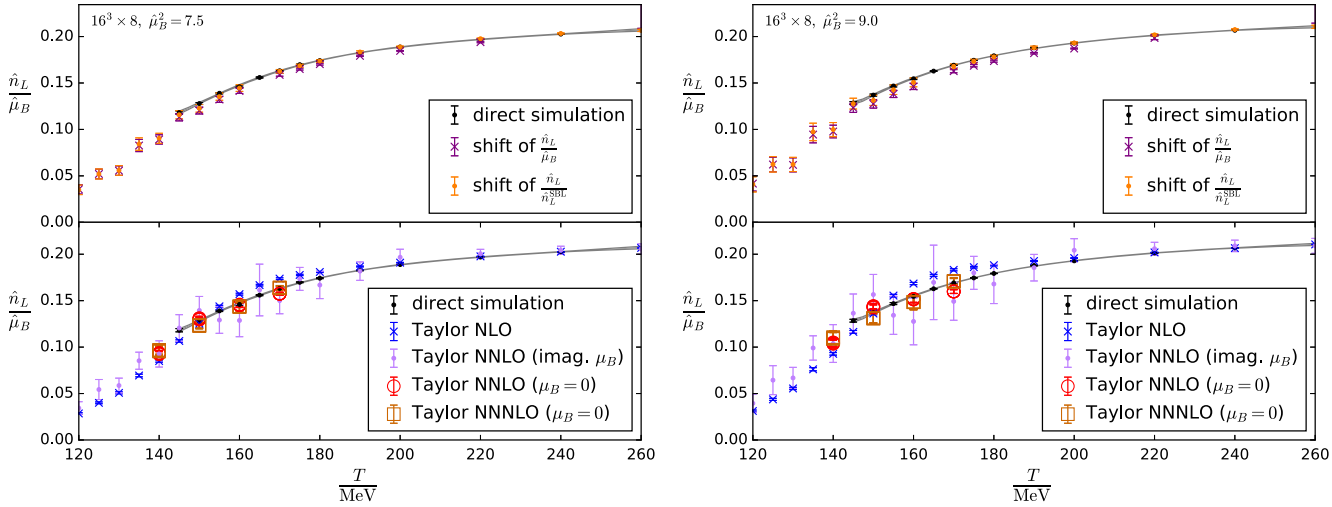

FIG. 3. The density $\hat{n}_L$ as a function of T for $\hat{\mu}_B = \sqrt{7.5}$ (left) and $\hat{\mu}_B = 3$ (right) for the Taylor expansion (bottom) and the resummation schemes based on shifting $\hat{n}_L/\hat{\mu}_B$ and $\hat{n}_L/\hat{n}_L^{\rm SBL}$ (top). The direct Taylor data from $\mu_B = 0$ simulations has smaller errors than the fit to imaginary μ_B data, due to the small volume in our study. For larger volumes, the signal-to-noise ratio of the direct p_6 and p_8 would be larger. A spline interpolation of the direct results is included to lead the eye.

simply related to the Lee-Yang zeros and may provide stronger limitations on convergence. While the lattice action used in this study is often used as a point in continuum extrapolations for QCD thermodynamics at zero baryon density, the size of cutoff effects at nonzero baryon density are not known at present. Thus, while there is a reasonable hope that observations made here about the convergence properties of different expansions carry over to the QCD continuum, this is not guaranteed and requires further investigations. In particular, rooted staggered fermions may lead to spurious singularities in the complex μ plane [60]. Thus, results with other discretizations would be welcome.

An obvious challenge is to extend the range of validity of the methods studied here to lower T and higher $\hat{\mu}_B$, so that the transition line [15,30,33,63,64] and the location of the conjectured critical end point [65–70] can be studied. Of course, the continuum and infinite volume limits will also have to be taken eventually.

ACKNOWLEDGMENTS

The project was supported by the BMBF Grant No. 05P21PXFCA. This work is also supported by the MKW NRW under the funding code NW21-024-A. Further funding was received from the DFG under the Project No. 496127839. This work was also supported by the Hungarian National Research, Development and Innovation Office, NKFIH Grant No. KKP126769. A. P. is supported by the J. Bolyai Research Scholarship of the Hungarian Academy of Sciences and by the ÚNKP-21-5 New National Excellence Program of the Ministry for Innovation and Technology. The authors gratefully acknowledge the Gauss Centre for Supercomputing e.V. (www.gauss-centre.eu) for funding this project by providing computing time on the GCS Supercomputers Jureca/Juwels at Juelich Supercomputer Centre, HAWK at Höchstleistungsrechenzentrum Stuttgart, and SuperMUC at Leibniz Supercomputing Centre.

[1] I. Montvay and G. Münster, *Quantum Fields on a Lattice*, Cambridge Monographs on Mathematical Physics (Cambridge University Press, Cambridge, England, 1997).
[2] Y. Aoki, G. Endrődi, Z. Fodor, S. D. Katz, and K. K. Szabó, Nature (London) **443**, 675 (2006).
[3] S. Borsányi, Z. Fodor, C. Hoelbling, S. D. Katz, S. Krieg, C. Ratti, and K. K. Szabó (Wuppertal-Budapest Collaboration), J. High Energy Phys. 09 (2010) 073.
[4] A. Bazavov *et al.*, Phys. Rev. D **85**, 054503 (2012).
[5] S. Borsányi, G. Endrődi, Z. Fodor, A. Jakovác, S. D. Katz, S. Krieg, C. Ratti, and K. K. Szabó, J. High Energy Phys. 11 (2010) 077.
[6] A. Bazavov *et al.* (HotQCD Collaboration), Phys. Rev. D **90**, 094503 (2014).
[7] R. V. Gavai and S. Gupta, Phys. Rev. D **68**, 034506 (2003).
[8] C. R. Allton, M. Doring, S. Ejiri, S. J. Hands, O. Kaczmarek, F. Karsch, E. Laermann, and K. Redlich, Phys. Rev. D **71**, 054508 (2005).
[9] S. Basak *et al.* (MILC Collaboration), Proc. Sci. LATTICE2008 (**2008**) 171 [arXiv:0910.0276].
[10] S. Borsányi, Z. Fodor, S. D. Katz, S. Krieg, C. Ratti, and K. Szabó, J. High Energy Phys. 01 (2012) 138.
[11] S. Borsányi, G. Endrődi, Z. Fodor, S. Katz, S. Krieg, C. Ratti, and K. K. Szabó, J. High Energy Phys. 08 (2012) 053.
[12] R. Bellwied, S. Borsányi, Z. Fodor, S. D. Katz, A. Pásztor, C. Ratti, and K. K. Szabó, Phys. Rev. D **92**, 114505 (2015).
[13] H. T. Ding, S. Mukherjee, H. Ohno, P. Petreczky, and H. P. Schadler, Phys. Rev. D **92**, 074043 (2015).
[14] A. Bazavov *et al.*, Phys. Rev. D **95**, 054504 (2017).
[15] A. Bazavov *et al.* (HotQCD Collaboration), Phys. Lett. B **795**, 15 (2019).
[16] M. Giordano and A. Pásztor, Phys. Rev. D **99**, 114510 (2019).
[17] A. Bazavov *et al.*, Phys. Rev. D **101**, 074502 (2020).
[18] P. de Forcrand and O. Philipsen, Nucl. Phys. **B642**, 290 (2002).
[19] M. D'Elia and M. P. Lombardo, Phys. Rev. D **67**, 014505 (2003).
[20] M. D'Elia and F. Sanfilippo, Phys. Rev. D **80**, 014502 (2009).
[21] P. Cea, L. Cosmai, and A. Papa, Phys. Rev. D **89**, 074512 (2014).
[22] C. Bonati, P. de Forcrand, M. D'Elia, O. Philipsen, and F. Sanfilippo, Phys. Rev. D **90**, 074030 (2014).
[23] P. Cea, L. Cosmai, and A. Papa, Phys. Rev. D **93**, 014507 (2016).
[24] C. Bonati, M. D'Elia, M. Mariti, M. Mesiti, F. Negro, and F. Sanfilippo, Phys. Rev. D **92**, 054503 (2015).
[25] R. Bellwied, S. Borsányi, Z. Fodor, J. Günther, S. D. Katz, C. Ratti, and K. K. Szabó, Phys. Lett. B **751**, 559 (2015).
[26] M. D'Elia, G. Gagliardi, and F. Sanfilippo, Phys. Rev. D **95**, 094503 (2017).
[27] J. N. Günther, R. Bellwied, S. Borsányi, Z. Fodor, S. D. Katz, A. Pásztor, C. Ratti, and K. K. Szabó, Nucl. Phys. **A967**, 720 (2017).
[28] P. Alba *et al.*, Phys. Rev. D **96**, 034517 (2017).
[29] V. Vovchenko, A. Pásztor, Z. Fodor, S. D. Katz, and H. Stoecker, Phys. Lett. B **775**, 71 (2017).
[30] C. Bonati, M. D'Elia, F. Negro, F. Sanfilippo, and K. Zambello, Phys. Rev. D **98**, 054510 (2018).
[31] S. Borsányi, Z. Fodor, J. N. Günther, S. K. Katz, K. K. Szabó, A. Pásztor, I. Portillo, and C. Ratti, J. High Energy Phys. 10 (2018) 205.
[32] R. Bellwied, S. Borsányi, Z. Fodor, J. N. Günther, J. Noronha-Hostler, P. Parotto, A. Pásztor, C. Ratti, and J. M. Stafford, Phys. Rev. D **101**, 034506 (2020).

[33] S. Borsányi, Z. Fodor, J. N. Günther, R. Kara, S. D. Katz, P. Parotto, A. Pásztor, C. Ratti, and K. K. Szabó, Phys. Rev. Lett. **125**, 052001 (2020).
[34] S. Borsányi, Z. Fodor, J. N. Günther, R. Kara, S. D. Katz, P. Parotto, A. Pásztor, C. Ratti, and K. K. Szabó, Phys. Rev. Lett. **126**, 232001 (2021).
[35] S. Mondal, S. Mukherjee, and P. Hegde, Phys. Rev. Lett. **128**, 022001 (2022).
[36] S. Mitra, P. Hegde, and C. Schmidt, Phys. Rev. D **106**, 034504 (2022).
[37] D. Bollweg, J. Goswami, O. Kaczmarek, F. Karsch, S. Mukherjee, P. Petreczky, C. Schmidt, and P. Scior (HotQCD Collaboration), Phys. Rev. D **105**, 074511 (2022).
[38] S. Borsanyi, Z. Fodor, J. N. Guenther, R. Kara, P. Parotto, A. Pasztor, C. Ratti, and K. K. Szabo, Phys. Rev. D **105**, 114504 (2022).
[39] M. Giordano, K. Kapás, S. D. Katz, D. Nógrádi, and A. Pásztor, J. High Energy Phys. 05 (2020) 088.
[40] S. Borsanyi, Z. Fodor, M. Giordano, S. D. Katz, D. Nogradi, A. Pasztor, and C. H. Wong, Phys. Rev. D **105**, L051506 (2022).
[41] Y. Aoki, Z. Fodor, S. D. Katz, and K. K. Szabó, Phys. Lett. B **643**, 46 (2006).
[42] G. S. Bali, F. Bruckmann, G. Endrődi, Z. Fodor, S. D. Katz, S. Krieg, A. Schäfer, and K. K. Szabó, J. High Energy Phys. 02 (2012) 044.
[43] G. S. Bali, F. Bruckmann, G. Endrődi, Z. Fodor, S. D. Katz, and A. Schäfer, Phys. Rev. D **86**, 071502 (2012).
[44] S. Borsányi, Z. Fodor, S. D. Katz, A. Pásztor, K. K. Szabó, and C. Török, J. High Energy Phys. 04 (2015) 138.
[45] B. B. Brandt, G. Endrődi, and S. Schmalzbauer, Phys. Rev. D **97**, 054514 (2018).
[46] M. D'Elia, F. Negro, A. Rucci, and F. Sanfilippo, Phys. Rev. D **100**, 054504 (2019).
[47] I. M. Barbour, S. E. Morrison, E. G. Klepfish, J. B. Kogut, and M.-P. Lombardo, Nucl. Phys. B, Proc. Suppl. **60**, 220 (1998).
[48] Z. Fodor and S. D. Katz, Phys. Lett. B **534**, 87 (2002).
[49] Z. Fodor and S. D. Katz, J. High Energy Phys. 03 (2002) 014.
[50] Z. Fodor and S. D. Katz, J. High Energy Phys. 04 (2004) 050.
[51] M. Giordano, K. Kapas, S. D. Katz, D. Nogradi, and A. Pasztor, Phys. Rev. D **102**, 034503 (2020).
[52] P. de Forcrand, S. Kim, and T. Takaishi, Nucl. Phys. B, Proc. Suppl. **119**, 541 (2003).
[53] A. Alexandru, M. Faber, I. Horváth, and K.-F. Liu, Phys. Rev. D **72**, 114513 (2005).
[54] Z. Fodor, S. D. Katz, and C. Schmidt, J. High Energy Phys. 03 (2007) 121.
[55] G. Endrődi, Z. Fodor, S. D. Katz, D. Sexty, K. K. Szabó, and C. Török, Phys. Rev. D **98**, 074508 (2018).
[56] A. Hasenfratz and D. Toussaint, Nucl. Phys. **B371**, 539 (1992).
[57] C. Morningstar and M. J. Peardon, Phys. Rev. D **69**, 054501 (2004).
[58] Y. Aoki, S. Borsányi, S. Durr, Z. Fodor, S. D. Katz, S. Krieg, and K. K. Szabó, J. High Energy Phys. 06 (2009) 088.
[59] J. B. Kogut and D. K. Sinclair, Phys. Rev. D **66**, 034505 (2002).
[60] M. Giordano, K. Kapas, S. D. Katz, D. Nogradi, and A. Pasztor, Phys. Rev. D **101**, 074511 (2020); **104**, 119901(E) (2021).
[61] S. Mukherjee, F. Rennecke, and V. V. Skokov, Phys. Rev. D **105**, 014026 (2022).
[62] P. Dimopoulos, L. Dini, F. Di Renzo, J. Goswami, G. Nicotra, C. Schmidt, S. Singh, K. Zambello, and F. Ziesché, Phys. Rev. D **105**, 034513 (2022).
[63] A. Pásztor, Z. Szép, and G. Markó, Phys. Rev. D **103**, 034511 (2021).
[64] N. Haque and M. Strickland, Phys. Rev. C **103**, 031901 (2021).
[65] K. Fukushima, Phys. Rev. D **77**, 114028 (2008); **78**, 039902 (E) (2008).
[66] P. Kovács, Z. Szép, and G. Wolf, Phys. Rev. D **93**, 114014 (2016).
[67] P. Isserstedt, M. Buballa, C. S. Fischer, and P. J. Gunkel, Phys. Rev. D **100**, 074011 (2019).
[68] W.-j. Fu, J. M. Pawlowski, and F. Rennecke, Phys. Rev. D **101**, 054032 (2020).
[69] F. Gao and J. M. Pawlowski, Phys. Lett. B **820**, 136584 (2021).
[70] J. Bernhardt, C. S. Fischer, P. Isserstedt, and B.-J. Schaefer, Phys. Rev. D **104**, 074035 (2021).